Aerosol Background Concentrations Influence Aerosol-Cloud Interactions as Much as the Choice of Aerosol-Cloud Parameterization

Louis Marelle, Gunnar Myhre, Jennie L Thomas, Jean-Christophe Raut

Geophysical Research Letters

RESEARCH LETTER
10.1029/2024GL111780

Key Points:

- Four aerosol-cloud parameterizations tested in a regional model are consistent with observed cloud changes during the 2014 Holuhraun eruption
- Liquid water path (LWP) observations during the eruption are not enough to exclude large LWP adjustments in models
- Aerosol radiative impacts are as sensitive to background aerosols as to aerosol-cloud interactions parameterization choice

Supporting Information:

Supporting Information may be found in the online version of this article.

Correspondence to:

L. Marelle,
louis.marelle@latmos.ipsl.fr

Citation:

Marelle, L., Myhre, G., Thomas, J. L., & Raut, J.-C. (2025). Aerosol background concentrations influence aerosol-cloud interactions as much as the choice of aerosol-cloud parameterization. *Geophysical Research Letters*, *52*, e2024GL111780. https://doi.org/10.1029/2024GL111780

Received 14 AUG 2024
Accepted 2 FEB 2025

Author Contributions:

Conceptualization: Louis Marelle, Gunnar Myhre
Data curation: Louis Marelle
Formal analysis: Louis Marelle
Funding acquisition: Louis Marelle, Gunnar Myhre, Jennie L. Thomas, Jean-Christophe Raut
Investigation: Louis Marelle, Gunnar Myhre, Jennie L. Thomas, Jean-Christophe Raut
Methodology: Louis Marelle, Gunnar Myhre, Jennie L. Thomas, Jean-Christophe Raut
Project administration: Gunnar Myhre, Jennie L. Thomas, Jean-Christophe Raut

Aerosol Background Concentrations Influence Aerosol-Cloud Interactions as Much as the Choice of Aerosol-Cloud Parameterization

Louis Marelle[1], Gunnar Myhre[2], Jennie L. Thomas[3], and Jean-Christophe Raut[1]

[1]Sorbonne Université, UVSQ, CNRS, LATMOS, Paris, France, [2]Center for International Climate Research, Oslo, Norway, [3]Université Grenoble Alpes, CNRS, IRD, Grenoble INP, IGE, Grenoble, France

Abstract We use an independent observational estimate of aerosol-cloud interactions (ACI) during the 2014 Holuhraun volcanic eruption in Iceland to evaluate four ACI parameterizations in a regional model. All parameterizations reproduce the observed pattern of liquid cloud droplet size reduction during the eruption, but strongly differ on its magnitude and on the resulting effective radiative forcing (ERF). Our results contradict earlier findings that this eruption could be used to constrain liquid water path (LWP) adjustments in models, except to exclude extremely high LWP adjustments of more than 20 $g\ m^{-2}$. The modeled ERF is very sensitive to the non-volcanic background aerosol concentration: doubling the non-volcanic aerosol background weakens the ACI ERF by ∼30%. Since aerosol biases in climate models can be an order of magnitude or more, these results suggest that aerosol background concentrations could be a major and under-examined source of uncertainty for modeling ACI.

Plain Language Summary Particles suspended in the atmosphere (aerosols) play a key role in cloud formation. These aerosol-cloud interactions have a major but uncertain influence on climate. We compare four different ways to calculate aerosol-cloud interactions in a numerical atmospheric model. We compare model results to observed changes in clouds measured from satellites during the Holuhraun eruption in Iceland in 2014, which released large amounts of volcanic gases forming atmospheric aerosols. We find that all four approaches reproduce the observed reduction in cloud droplet sizes during the eruption, but that they disagree on its intensity and its impacts on the Earth's energy budget. An earlier study found that aerosol-cloud interactions did not significantly increase the amount of liquid water in the clouds; using a more recent version of the satellite observations we find that large increases are possible. We also show that the eruption's impacts on the Earth's energy budget strongly depend on non-volcanic aerosols already present in the atmosphere: doubling non-volcanic aerosols reduces the impacts by ∼30%. Aerosol biases in climate models can be far greater, indicating that this could be a major source of uncertainty for aerosol-cloud interactions and for understanding past, present and future climates.

1. Introduction

In Earth's atmosphere, a liquid cloud droplet can only form on a preexisting aerosol serving as a cloud condensation nucleus (CCN). As a result, the abundance and properties of aerosols have a direct influence on the physical and optical properties of clouds, and ultimately on the radiative budget of the Earth, through a range of processes called aerosol-cloud interactions (ACI, e.g., Lohmann & Feichter, 2005). The effective radiative forcing of ACI is currently estimated at −0.8 W m^{-2}, with likely values ranging from −1.45 to −0.25 W m^{-2} (IPCC, 2023). Despite the importance of ACI forcing for climate, this very wide uncertainty range has not been reduced significantly in recent years, and ACI remain the main source of uncertainty for quantifying anthropogenic radiative forcing, and a key physical uncertainty in climate projections.

Aerosols have a cooling effect on the global climate, but clean air policies have helped reduce aerosol pollution in recent years. There is evidence that improvements in air quality have also reduced aerosol cooling globally, revealing more of the underlying greenhouse gas warming trend (Hodnebrog et al., 2024; Quaas et al., 2022). In the Arctic, a region particularly sensitive to climate change, this "unmasking" of greenhouse warming may have been responsible for +0.8°C of additional warming from 1990 to 2015, half of the anthropogenic warming trend during the same period (von Salzen et al., 2022). These trends will likely continue in the future because of further emission reductions. In order to improve climate projections and to understand past changes, and to inform the

Resources: Gunnar Myhre, Jennie L. Thomas
Software: Louis Marelle, Jean-Christophe Raut
Supervision: Gunnar Myhre, Jennie L. Thomas
Validation: Louis Marelle
Visualization: Louis Marelle
Writing – original draft: Louis Marelle, Jennie L. Thomas
Writing – review & editing: Louis Marelle, Gunnar Myhre, Jennie L. Thomas

policies that consider the trade-offs between short term and long term climate strategies, it is thus critical to better constrain the ACI forcing and the main causes of uncertainty between models.

The impacts of ACI are hard to constrain in models because of the complexity of the processes involved, from the underlying microphysical changes to the interactions with cloud-scale and large-scale dynamics (e.g., Lohmann et al., 2016). To the first order, increasing aerosol concentrations increases liquid cloud droplet numbers and reduces cloud droplet size, forming optically thicker clouds than in aerosol-poor conditions (Twomey, 1974). In order to represent this process, climate models use ACI parameterizations of varying complexities, but it is unclear how much this range of parameterizations influences the predicted ACI radiative forcing uncertainty (Ekman, 2014), or how to best evaluate them against observations.

In fact, modeled ACI are also difficult to evaluate because the effects of ACI are very hard to observe directly. It is possible to compare observations of polluted clouds from unpolluted clouds to find statistical relationships between aerosols and clouds. However, extracting the causal ACI signal from observational correlations is complicated by confounding factors (Gryspeerdt et al., 2019; D. T. McCoy, Field, et al., 2020; Mahfouz et al., 2024; Mülmenstädt et al., 2024), and requires sufficient data volume so that the signal from aerosol-cloud interactions could plausibly be detected. In addition, satellite data sets have limited sensitivity to cloud microphysics and are not currently able to estimate vertically resolved aerosol concentrations inside clouds (Quaas et al., 2020). Furthermore, due to the magnitude of anthropogenic and natural emissions of aerosols and their precursors, it is not feasible either to conduct controlled field experiments, such as emitting large enough amounts of aerosols during a long enough period. Large volcanic eruptions can be thought of as rare natural opportunistic experiments that can help us circumvent this problem (Christensen et al., 2022).

The Holuhraun fissure eruption in Iceland, from late August 2014 to February 2015, emitted the equivalent of 2 years of the European Union's anthropogenic SO_2 emissions in just 6 months (EEA, 2014; Pfeffer et al., 2018), with most of the emissions occurring during the first 2 months of the eruption. During this time, observed cloud droplet sizes in the North Atlantic were reduced far outside the range of natural variability, due to ACI from volcanic aerosols (D. T. McCoy & Hartmann, 2015). This independent observational estimate of ACI was compared previously to the predictions of climate models, showing that several models were inconsistent with observations (Malavelle et al., 2017; D. T. McCoy et al., 2018).

In this study, we compare observed ACI in liquid clouds during the Holuhraun eruption against the predictions of 4 different ACI parameterizations in the same model framework. Specifically, we evaluate how well the different ACI parameterizations reproduce observed liquid cloud changes during the 2014 Holuhraun eruption, we quantify the uncertainty range in ACI radiative effect resulting from the choice of parameterization, and we compare this parameterization uncertainty to the uncertainty due to aerosol biases in the model. We show that the background aerosol concentration is a critical factor for modeling ACI accurately, and we discuss the wider implications for radiative forcing and climate modeling in the conclusion.

2. Methods

2.1. WRF-Chem 4.3.3 Model

We perform simulations with the Weather Research and Forecasting model including chemistry (WRF-Chem, Grell et al., 2005), starting on 2014-08-15 and ending on 2014-11-01, allowing for 2 weeks of initial spin-up before the start of the eruption on 2014-08-29. The simulation domain is approximately 6,000 km × 6,000 km in size, and centered on Iceland. The horizontal resolution is 50 km × 50 km with 72 vertical levels between the surface and 50 hPa.

All simulations are performed with WRF-Chem version 4.3.3, including optimizations for polar regions described in Marelle et al. (2017). New model updates since Marelle et al. (2017) are described below, including ACI developments presented in Section 2.1.4.

2.1.1. WRF-Chem Chemistry-Aerosol Setup

Within WRF-Chem, we use the MOZART gas-phase chemistry mechanism (Emmons et al., 2010), and the MOSAIC-4bin sectional aerosol model (Zaveri et al., 2008) including aqueous chemistry (a setup called MOZART-MOSAIC-4BIN-AQ in WRF-Chem). Initial and time-varying boundary conditions for trace gases and

aerosols are from the CAM-Chem model (Buchholz et al., 2019). For this study, we also update the dimethylsulfide (DMS) chemistry scheme in MOZART-MOSAIC-4BIN-AQ to von Glasow and Crutzen (2004). The updated DMS mechanism includes methanesulfonic acid (MSA) aerosols and the associated heterogeneous chemistry. It was partly implemented in WRF-Chem for the CBM-Z and CRIMECH mechannisms by Archer-Nicholls et al. (2014); we include it fully in MOZART-MOSAIC-4BIN-AQ.

2.1.2. WRF-Chem Meteorological Setup

The model meteorology is calculated during the simulation, with 2-way coupling between meteorology, chemistry and aerosols. In our simulations, grid-scale cloud microphysics are modeled by the 2-moment Thompson Aerosol-Aware scheme (Thompson & Eidhammer, 2014), and subgrid clouds by the Grell-3 cumulus scheme (Grell & Dévényi, 2002). We modified the cloud fraction diagnosis in WRF-Chem to follow Xu and Randall (1996). The initial and time-varying (6 hr) boundary conditions for meteorology are taken from the ERA5 reanalysis (Copernicus Climate Change Service, 2017), and spectral nudging to ERA5 is applied for wind and temperature features over the 700 km scale. The full meteorological setup is provided in Table S1 in Supporting Information S1.

2.1.3. Emissions Used in WRF-Chem Simulations

Daily varying volcanic SO_2 emissions and plume emission heights for the Holuhraun eruption are from Pfeffer et al. (2018). Emissions are injected in WRF-Chem as a uniform source from the provided plume bottom altitude to plume top, at the location of the eruption (64.87°N, 16.84°W). 1% of SO_2 emissions are emitted as primary sulfate (Ilyinskaya et al., 2017).

Anthropogenic emissions are from the CAMSv4.2 inventory (van der Gon et al., 2023), applying sector-dependent daily and hourly emission variations and vertical profiles (Archer-Nicholls et al., 2014; Denier van der Gon et al., 2011). 3% of anthropogenic SO_x is emitted as primary sulfate (Alexander et al., 2009). Open biomass burning emissions are from FINNv1.5 (Wiedinmyer et al., 2014).

Natural sea spray emissions from open oceans follow Ioannidis et al. (2023) but do not include experimental emissions of marine organics. Dust emissions are included (Chin et al., 2002), but are very low in the domain. Terrestrial biogenic emissions are from MEGANv2.1 (Guenther et al., 2012), and DMS emissions use the ocean climatology of Lana et al. (2011) with the sea-air flux from Nightingale et al. (2000).

2.1.4. Aerosol-Cloud Parameterizations Implemented and Compared in WRF-Chem

We compare four aerosol-cloud interaction parameterizations in the WRF-Chem model:

- TE14: The ACI parameterization of the Thompson aerosol-aware cloud model (Thompson & Eidhammer, 2014) calculates cloud droplet and cloud ice crystal formation based on the thermodynamical conditions in the clouds and two aerosol parameters, the water-friendly and ice-friendly aerosol number concentrations. In the base version of the model, TE14 initializes these aerosol numbers from a fixed climatology. Here, TE14 uses aerosol numbers predicted by WRF-Chem. The water-friendly aerosol is set as the hydrophilic volume fraction (sulfate, nitrate, ammonium, sea salt, MSA) of the total WRF-Chem aerosol number in each size bin. To eliminate a source of variability between simulations, ice-friendly aerosol numbers are set to the fixed minimum model value of 5 L^{-1}. This is consistent with the negligible emission of ice-active volcanic dust in the eruption, and with the low ice nucleating particle numbers at high latitudes (Li et al., 2022).
- ARG02: The parameterization of Abdul-Razzak and Ghan (2002) calculates aerosol activation and cloud droplet numbers based on aerosol size, number, and hygroscopicity in each size bin. It was already included in the WRF-Chem chemistry code as part of the Morrison and Lin microphysic schemes. We reimplemented ARG02 into Thompson microphysics, consistently with TE14. For consistency, both TE14 and ARG02 include the same sub-grid distribution of updraft velocity from Ghan et al. (1997).
- BL95: The parameterization of Boucher and Lohmann (1995) predicts cloud droplet number concentrations as a function of accumulation-mode sulfate mass. We include it in WRF-Chem by overwriting the cloud droplet number passed by Thompson microphysics to the radiation code by the BL95-predicted value.

- LMDZ6: This parameterization, based on BL95, is used in the LMDZ6 climate model (Madeleine et al., 2020), and predicts cloud droplet number concentrations as a function of accumulation-mode soluble mass. The implementation is the same as in BL95, using the WRF-Chem mass of sulfate, ammonium, and sea salt. The LMDZ6 model does not include nitrate or MSA, so these were not used for the calculation.

By design, LMDZ6 and BL95 only represent the effect of aerosols on cloud droplet number and radiation, the so-called "first indirect effect" (Twomey, 1974), while ARG02 and TE14 are also able to represent microphysical adjustments of clouds to ACI, influencing precipitation, cloud dynamics and lifetime, and liquid water path, the "second indirect effect" (Albrecht, 1989).

For each of these four ACI parameterizations, we perform a control simulation (VOLC) that includes volcanic emissions, and a counterfactual simulation (noVOLC) without volcanic emissions, for a total of eight simulations. The difference VOLC-noVOLC is used to estimate the effect of ACI due to volcanic aerosols. In order to further reduce differences between simulations, only the ARG02 simulation is run as a fully coupled WRF-Chem simulation with prognostic aerosols. TE14, LMDZ6 and BL95 aerosols are instead forced by the 3-hourly aerosol fields produced by ARG02. Furthermore, to remove the contribution of direct aerosol-radiation interactions (ARI) from the VOLC-noVOLC signal, all eight simulations include simplified direct ARI from identical climatological aerosol fields (Tegen et al., 1997), instead of using prognostic WRF-Chem aerosols. This workflow also has the advantage of speeding up the calculations significantly, allowing for the sensitivity simulations presented in Section 3.4. But the main advantage is that all four ACI setups use the exact same meteorological setup, ARI, ice nucleation scheme, and aerosol fields for liquid cloud ACI, ensuring that the only difference between them is the choice of the liquid-cloud ACI parameterization.

2.2. MODIS Observations of Clouds for Evaluating Modeled ACI

We estimate the effect of the eruption on cloud properties using observations from the MODIS instruments on board the Aqua and Terra satellites, using the $1° \times 1°$ monthly gridded cloud products MYD08_M3_6_1 and MOD08_M3_6_1. Specifically, we compute the October 2014 MODIS liquid effective radius (r_{eff}) and liquid water path (LWP) anomalies from the October 2002–2022 climatological baseline (excluding 2014). We choose these specific variables for consistency with previous studies such as Malavelle et al. (2017), and because r_{eff} and the 3D liquid water content are the variables used to calculate the radiative effect of liquid clouds within WRF-Chem's radiative transfer model.

For a like-for-like comparison of MODIS and WRF-Chem, WRF-Chem r_{eff} and LWP are postprocessed to follow the MODIS monthly L3 product procedure (Hubanks et al., 2016). Cloud properties are extracted from the 3-hourly WRF-Chem output, keeping only daytime scenes with solar zenith angles less than 81.373°, producing daily maps, which are then aggregated to monthly gridded maps of r_{eff} and LWP. To our knowledge, Malavelle et al. (2017) did not apply such screening to their model results, which could bias their analysis. MODIS in-cloud LWP is compared with WRF-Chem's grid-scale LWP by multiplying the in-cloud values with the liquid cloud fraction. Regionally averaged comparisons in Section 3 are taken over ocean points only, from latitudes 47°N to 77°N, longitudes 60°W to 30°E, with area-weighted averaging.

3. Results

3.1. Effect of the Eruption on the Cloud Droplet Radius, and Sensitivity to ACI Parameterization

In October 2014, during the Holuhraun eruption, the MODIS cloud r_{eff} was significantly smaller than usual. On average in the North Atlantic, the effective radius anomaly $\Delta r_{eff} = -1.48 \mu m$ (Figure 1), outside two standard deviations of the climatology ($2\sigma = 1.14\ \mu m$). This is a consequence of ACI from the additional volcanic aerosols (Malavelle et al., 2017).

The 4 ACI parameterizations predict a strong r_{eff} reduction in the domain, and reproduce the overall geographical pattern of this change. We do not expect a perfect agreement between observations and models, since MODIS r_{eff} retrievals are themselves biased at the high solar zenigh angles found in October at high latitudes (Grosvenor & Wood, 2014), although this bias is relatively low, −5% at highest angles. The modeled Δr_{eff} is sensitive to the choice of ACI parameterization, with $-1.20\ \mu m$, $-1.63\ \mu m$, $-1.09\ \mu m$ and $-0.66\ \mu m$ for ARG02, TE14, BL95, and LMDZ6 respectively (Table S2 in Supporting Information S1). The simple BL95 parameterization predicts a

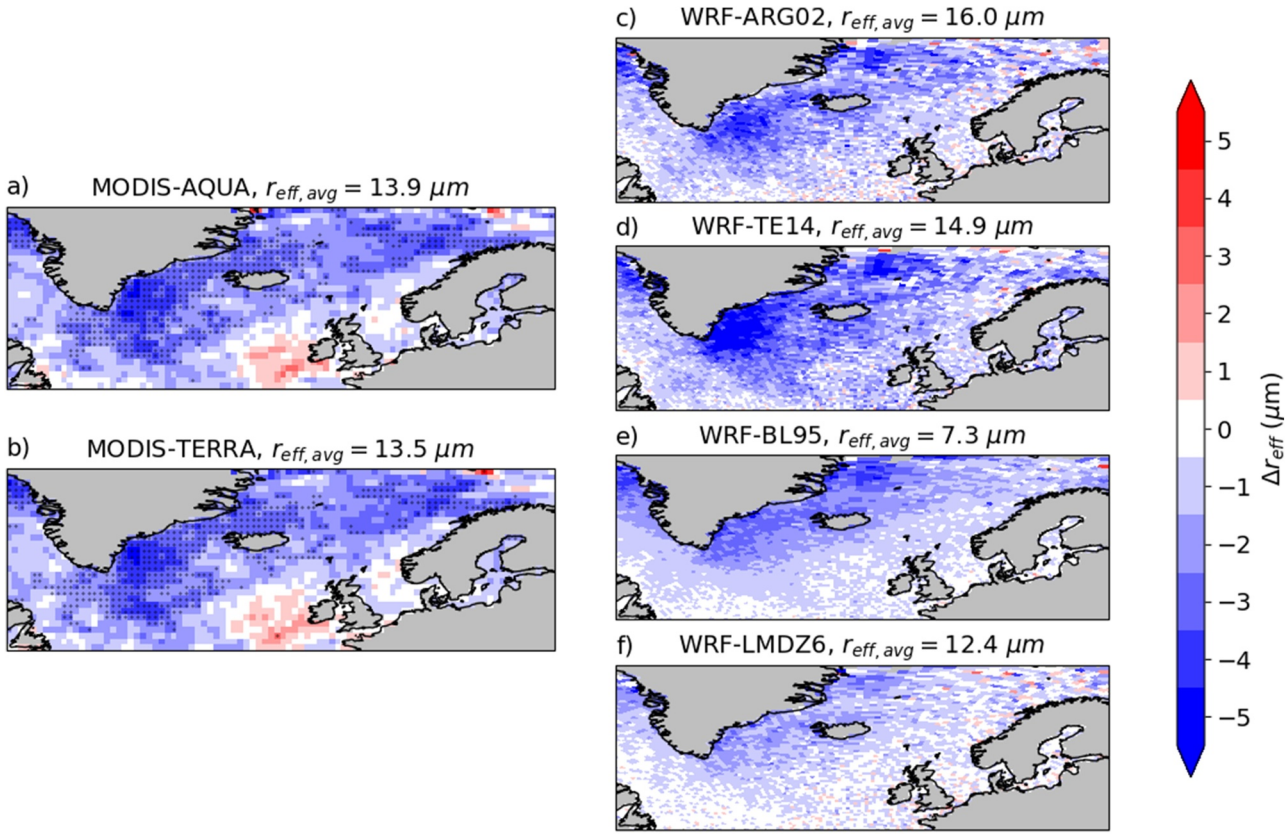

Figure 1. Cloud liquid droplet effective radius response to volcanic aerosols. (a) MODIS-AQUA and (b) MODIS-Terra liquid cloud droplet effective radius anomaly in October 2014, 2002–2022 baseline. (c–f) WRF-Chem liquid cloud droplet effective radius anomaly due to volcanic emissions (VOLC—noVOLC anomaly, October 2014 average) using the (c) ARG02 (d) TE14 (e) BL95 and (f) LMDZ6 ACI parameterizations. Above each panel, $r_{eff,avg}$ gives the regionally averaged r_{eff} in October 2014, observed or modeled in the VOLC simulation.

reasonable Δr_{eff} anomaly, but strongly underestimates the observed absolute r_{eff} by −47%. Conversely, LMDZ6 reproduces the observed r_{eff} but strongly underestimates the observed Δr_{eff} by −55%. Implications for radiative forcing in LMDZ6 are discussed in Section 3.3. LMDZ6 and BL95 are simple empirical parameterizations predicting cloud droplet number from aerosol mass. It is likely that in such parameterizations there is a trade-off between correctly reproducing the absolute r_{eff} or the Δr_{eff}.

Three of the four parameterizations (ARG02, BL95, LMDZ6) underestimate Δr_{eff}. This could be a limitation of the ACI parameterizations themselves, or it could be due to underestimated aerosols in the volcanic plume. During the eruption, the WRF-ARG02 simulation reproduces the observations of fine particle mass concentration ($PM_{2.5}$) at European surface sites very well (Figure S1a in Supporting Information S1). Before the start of the eruption, background aerosol sulfate is also well represented, but after the eruption begins in late August, the model underestimates sulfate at surface sites (Figure S1b in Supporting Information S1). To our knowledge, the vertical distribution of aerosols in the Holuhraun plume was not observed, so it is not clear if the same bias is present at higher altitudes where aerosols interact with clouds, or if it could be due to errors in the downward mixing of the volcanic plume into the boundary layer. In addition, emission amounts from the eruption are also uncertain (Schmidt et al., 2015), and our choice of emission inventory could contribute to model biases. In the following, we will focus on the sensitivity of ACI to parameterizations and aerosols in the model.

3.2. Effect of the Eruption on the Liquid Water Path, and Sensitivity to ACI Parameterization

Figure 2 compares the observed and modeled LWP anomaly due to the eruption in October 2014. WRF-ARG02 and WRF-TE14 show a weak regionally averaged ΔLWP response of +3.9 g m^{-2} and +6.8 g m^{-2}) respectively (Table S2 in Supporting Information S1), well below the threshold of observed natural

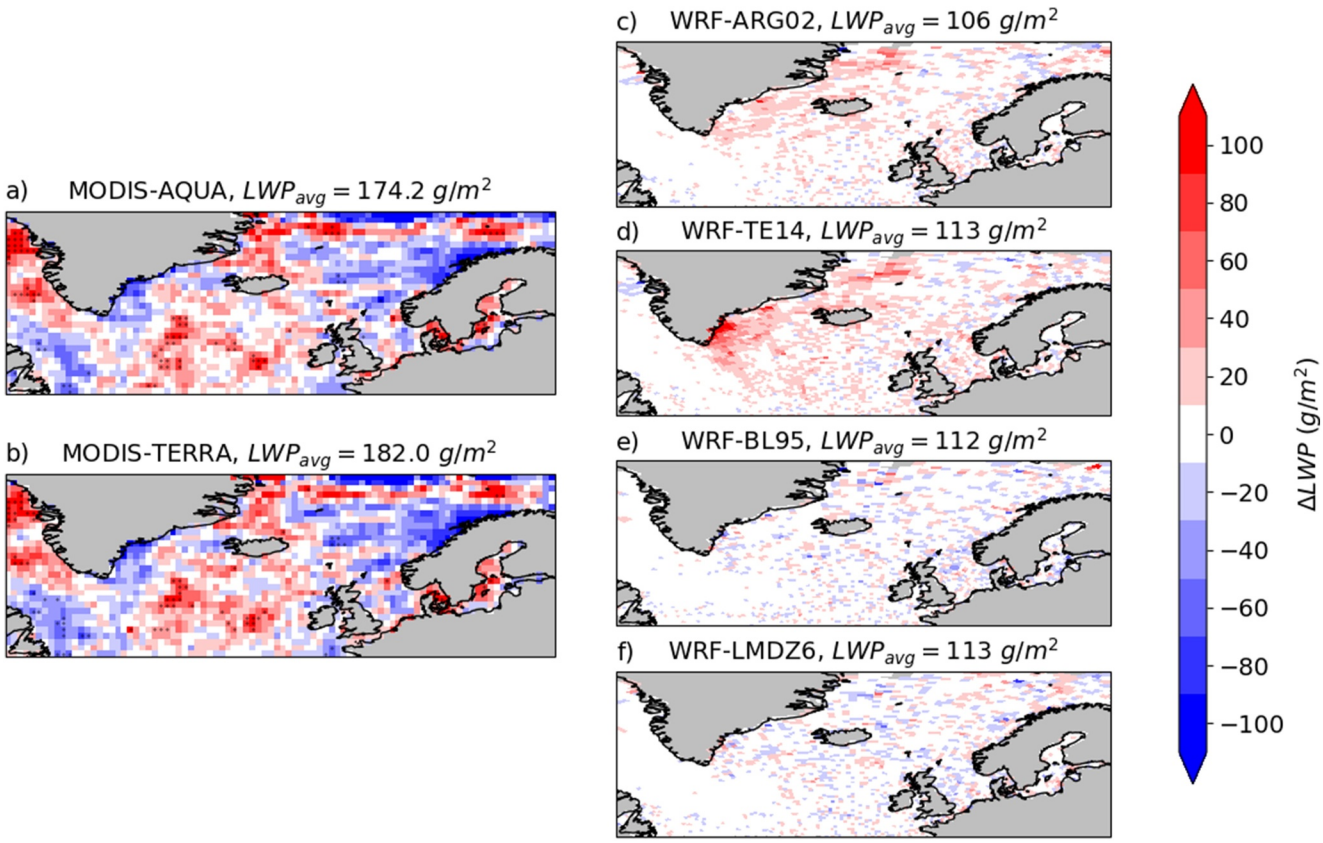

Figure 2. Liquid water path response to volcanic aerosols. (a) MODIS-AQUA and (b) MODIS-Terra liquid water path radius anomaly observed in October 2014, 2002–2022 baseline. (c–f) WRF-Chem liquid water path anomaly due to volcanic emissions (VOLC—NOVOLC anomaly), October 2014 average, using the (b) ARG02 (c) TE14 (d) BL95 and (e) LMDZ6 ACI parameterizations. BL95 and LMDZ6 do not include the second indirect effect.

variability ($2\sigma = 19.3$ g m^{-2}). It is important to note that BL95 and LMDZ6 do not include cloud microphysical adjustments to the r_{eff} change (the second indirect effect). For BL95 and LMDZ6, LWP changes are then only due to random variability and small dynamical adjustments to the first indirect effect, and are as expected close to zero. The absolute regionally averaged LWP is close to 110 g m^{-2} with all parameterizations, significantly lower than MODIS observations (∼180 g m^{-2}), but higher than the climate model simulations in Malavelle et al. (2017) (mean LWP∼60 g m^{-2}).

Using MODIS products from version 5.1, Malavelle et al. (2017) found that the impact of the eruption on LWP was very limited, and could not exceed 9 g m^{-2}. They concluded that large LWP adjustments in climate models were inconsistent with these observations. Using revised LWP from MODIS version 6.1, and a longer climatological period (2002–2022 excluding 2014 instead of 2002–2013) we find a much larger significance threshold $2\sigma = 19.3$ g m^{-2}, which is consistent with even the largest climate model ΔLWP of 16.3 g m^{-2} from Malavelle et al. (2017).

A recent study suggested that the cloud response to the Holuhraun eruption could be dominated by cloud fraction adjustment, instead of changes in LWP or r_{eff} (Chen et al., 2022). This is not the case here, and WRF-ARG02 and WRF-TE14 predict positive but very small cloud fraction adjustments of +0.4% and +0.8% points respectively (Figure S2 and Table S2 in Supporting Information S1).

3.3. Sensitivity of the Aerosol Radiative Impact to the ACI Parameterization

The regionally averaged radiative effect of ACI on the net shortwave flux at top-of-atmosphere $\left(ERF_{aci}^{SW}\right)$ in October 2014 is −1.12, −1.97, −1.08, and −0.34 W m^{-2} for ARG02, TE14, BL95, and LMDZ6 respectively (Table S2 in Supporting Information S1). The weak −0.34 W m^{-2} ERF_{aci}^{SW} in LMDZ6 is consistent with its low

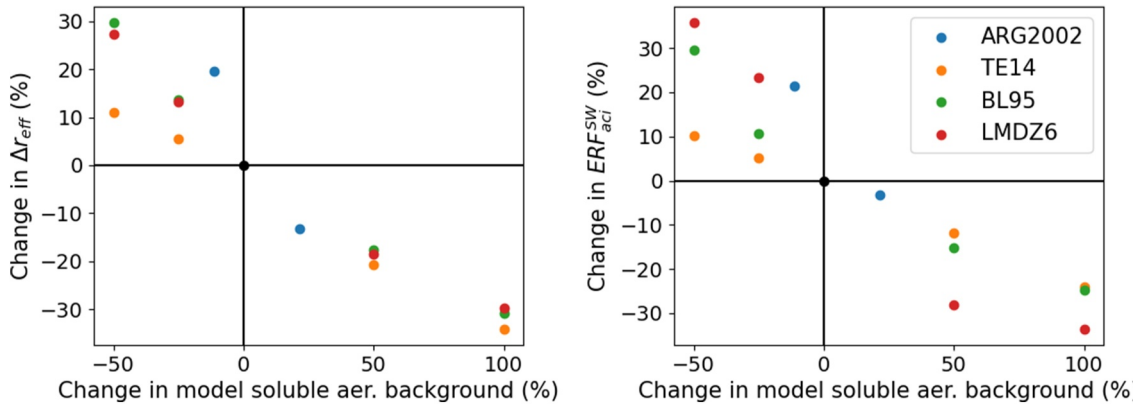

Figure 3. Sensitivity of volcanic aerosol-cloud-interactions to the non-volcanic aerosol background concentration. (left) effective radius anomaly during the eruption (right) indirect shortwave radiative effect of the eruption at top-of-atmosphere. All values are given as percentage changes from the unperturbed reference simulations.

Δr_{eff} response. This could explain why the IPSL-CM6 climate model, where LMDZ6 is hosted, has the weakest ACI effective radiative forcing among CMIP6 models (Zelinka et al., 2023). Despite very different approaches and complexities, ARG02 and BL95 predict a similar ERF^{SW}_{aci}. TE14, which best reproduces the observed r_{eff} and Δr_{eff}, also predicts the strongest forcing, nearly 2 times stronger than ARG02 and BL95.

3.4. Sensitivity of the Modeled Cloud Response to the Aerosol Background

Aerosol-cloud interactions are strongly non-linear. For this reason, the modeled radiative impact of an aerosol perturbation is sensitive to the absolute aerosol concentrations in the background state (Carslaw et al., 2013; Lohmann et al., 2000; I. L. McCoy, McCoy, et al., 2020). In order to estimate the sensitivity of the modeled ACI to the non-volcanic aerosol background, we perform sensitivity experiments in the WRF-Chem model by perturbing the non-volcanic aerosol climatology *aer* (units $\mu g\ kg^{-1}$ and kg^{-1}) used to force the TE14, LMDZ6, and BL95 parameterizations by a factor $\alpha = 0.5$, 0.75, 1.5, or 2.

$$aer_{NoVolc,perturbed} = \alpha \times aer_{NoVolc} \quad (1)$$

$$aer_{Volc,perturbed} = \alpha \times aer_{NoVolc} + (aer_{Volc} - aer_{NoVolc}) \quad (2)$$

For each sensitivity simulation, we calculate the VOLC-noVOLC Δr_{eff} and ERF^{SW}_{aci} and compare it to the value from the unperturbed reference run, as a function of the perturbation anomaly $\alpha - 1.0$, which is equal to zero for the unperturbed case. Aerosols cannot be perturbed directly in ARG02, because they are not forced but computed prognostically in the model. In order to estimate the sensitivity of ARG02 to background aerosol concentrations, we perturb instead the marine emissions of sea spray and DMS. Since these sensitivity simulations are fully coupled, they are computationally costly, and we only perform two sensitivity simulations with emissions multiplied by 0.5 and 2.

Figure 3 shows that the droplet effective radius and the aerosol forcing are very sensitive to the non-volcanic aerosol background. When the background aerosol concentration is doubled (+100%), the Δr_{eff} is ∼30%–35% weaker than in the reference run, and the ERF^{SW}_{aci} is ∼25%–35% weaker, even though the volcanic aerosol perturbation is exactly the same. When the background is divided by 2 (−50%), the Δr_{eff} is ∼10%–30% stronger than in the reference run, and the ERF^{SW}_{aci} is ∼10%–40% larger. Since local biases in aerosol background concentrations can often be an order of magnitude or more in climate models (e.g., Bian et al., 2024; Lapere et al., 2023), this effect could be a major source of uncertainty for radiative forcing calculations.

4. Discussion, Conclusions, and Recommendations for Climate Modeling

In this study, we compare four ACI parameterizations in the same regional modeling framework during a large volcanic eruption. We calculate the sensitivity of the cloud response and of the aerosol radiative forcing to the choice of parameterization, and the sensitivity of volcanic ACI to the non-volcanic aerosol background.

All four ACI parameterizations reproduce the pattern and overall magnitude of the observed changes in liquid cloud droplet effective radius during the eruption, but LMDZ6 underestimates these changes. Modeled ACI are sensitive to ACI parameterization in terms of effective radius and radiative impacts. The ACI radiative impact is very weak for the LMDZ6 ACI parameterization, and we believe that this choice of parameterization could explain the low aerosol ERF in the associated IPSL-CM6 climate model. We did not test the full parameterization panel from CMIP6 models, and our results certainly underestimate the full range of sensitivity to ACI parameterization; however, the types of parameterizations tested are representative of this generation of climate models.

Our study disagrees with one of the main conclusions of Malavelle et al. (2017): we find that this volcanic case study cannot be used to constrain the ACI LWP adjustment in climate models, except to rule out very high regional LWP changes of more than ∼20 g m^{-2}. These values are much larger than the magnitude of the LWP change due to ACI in WRF-Chem in either ARG02 or TE14 (∼5 g m^{-2}), and consistent with even the largest LWP changes predicted by climate models in Malavelle et al. (2017). Our simulations and those of Malavelle et al. (2017) underestimate the observed LWP in the region, so further work is needed to fully understand LWP adjustments in models.

We find that the modeled cloud response to the eruption is also very sensitive to the non-volcanic background aerosol concentration: a doubling of the aerosol background translates into a $\sim -30\%$ change in ACI radiative forcing. This sensitivity is worrying because biases in aerosol mixing ratio in climate models can be far greater. Allen and Landuyt (2014) found that model spread for black carbon aerosols in CMIP5 is up to two orders of magnitude in the free troposphere, and Lapere et al. (2023), Bian et al. (2024) showed that aerosol differences between models in the remote marine and polar troposphere, respectively, can be one or two orders of magnitude.

Twenty-five years ago, Lohmann et al. (2000) showed that aerosol-cloud radiative forcing in the ECHAM4 climate model was sensitive to the pre-industrial aerosol burden. Based on this result, Lohmann and Feichter (2005) suggested that the large differences in ERF_{ACI} between models could be due to "the dependence of the indirect aerosol effect on the background aerosol concentration." Carslaw et al. (2013) later found that uncertainties in natural emissions could account for 45% of the ERF_{ACI} uncertainty in a single global model. However, to our knowledge, the precise contribution of these errors to the large CMIP multimodel ERF_{ACI} uncertainty has not been investigated since, and was not identified as a major issue in recent efforts for understanding aerosol ERF (Bellouin et al., 2020; Fiedler et al., 2023; Mülmenstädt & Feingold, 2018; Quaas et al., 2020; Seinfeld et al., 2016). In light of our results and of earlier literature, we recommend a systematic analysis of how the natural aerosol background influences the ERF_{ACI} spread in climate models. If background aerosols are indeed important, improving the representation of natural aerosols such as sea-spray, sulfate from oceanic DMS, and biomass burning could be a more efficient pathway for reducing ACI uncertainties than difficult improvements in complex aerosol-cloud processes.

For this purpose, a detailed evaluation of aerosols in climate models is critical. ACI are determined by aerosol properties within clouds, and are especially sensitive to aerosol concentrations and aerosol size (Dusek et al., 2006). However, aerosols in climate models are usually evaluated in terms of vertically integrated bulk properties such as Aerosol Optical Depth (AOD), which is also the usual CCN proxy for observational estimates of the aerosol ERF (Bellouin et al., 2020; Gryspeerdt et al., 2023). This is concerning, because large errors in aerosol concentrations, vertical distributions, water uptake, and size distributions can compensate to give a reasonable AOD in models (Quaas et al., 2020). In this context, we also recommend routine evaluations and comparisons of aerosol vertical distributions in climate models, for example, using the now extensive LiDAR and aircraft measurement data sets.

The sensitivity of ACI to aerosol background is not just important in the pre-industrial period and for quantifying ERF_{ACI} in climate models, which has been the focus until now. Our results suggest that tackling these issues and improving the representation of background aerosols in models could also help us better understand the effect of ACI at shorter time scales, including the influence of ACI on specific extreme events, its effect on meteorological forecasts, and the effect of recent and future clean air policies on climate.

Data Availability Statement

We provide the updated WRF-Chem 4.3.3 model version used in this study as Marelle (2024a). The WRF preprocessing system (WPS) is available at https://archive.softwareheritage.org/swh:1:dir:21227ff84043afa53bb870245da4061fe7f0c7ab;origin=https://github.com/wrf-model/WPS;visit=swh:1:snp:096256316e752343901abad92a7dd9c2529f48cb;anchor=swh:1:rev:5a2ae63988e632405a4504cfb143ce7f0230a7a0. WRF-Chem preprocessor tools (mozbc, fire_emiss and bio_emiss) are available at https://www2.acom.ucar.edu/wrf-chem/wrf-chem-tools-community. We provide the WRF-Chem run and setup scripts, preprocessing codes, and post-processing codes created as Marelle (2024b). ERA5 input data on pressure and surface levels for WRF are published as Copernicus Climate Change Service (2017), and the CAM-Chem input data for initial and boundary conditions as Buchholz et al. (2019). CAMSv4.2 emissions are available at https://ads.atmosphere.copernicus.eu/datasets/cams-global-emission-inventories FINNv1.5 emissions are distributed at https://www.acom.ucar.edu/Data/fire/. The Lana DMS climatology can be found at https://www.bodc.ac.uk/solas_integration/implementation_products/group1/dms/documents/dmsclimatology.zip. MODIS satellite observations from the MYD08_M3_6_1 and MOD08_M3_6_1 products are published as Platnick et al. (2015a, 2015b). Observations of atmospheric composition used in the supplement are from https://ebas.nilu.no/.

Acknowledgments

This project has received funding from Horizon Europe programme under Grant 101137680 via project CERTAINTY (Cloud-aERosol inTeractions & their impActs IN The earth sYstem); from the European Union's Horizon 2020 research and innovation programme under Grant 101003826 via project CRiceS (Climate Relevant interactions and feedbacks: the key role of sea ice and Snow in the polar and global climate system); and from the project SUPER (no. 250573) funded through the Research Council of Norway. This research has been partly funded by French National Research Agency (ANR) via the project MPC2 (n° ANR-22-CEA01-0009-02). Computer analyses benefited from access to IDRIS HPC resources (GENCI allocations A011017141 and A013017141), and from the IPSL mesocenter ESPRI facility which is supported by CNRS, UPMC, Labex L-IPSL, CNES and Ecole Polytechnique. We acknowledge use of the WRF-Chem preprocessor tools mozbc, fire_emiss and bio_emiss provided by the Atmospheric Chemistry Observations and Modeling Lab (ACOM) of NCAR. We acknowledge ECCAD for the archiving and distribution of the CAMS emissions data.

References

Abdul-Razzak, H., & Ghan, S. J. (2002). A parameterization of aerosol activation 3. Sectional representation. *Journal of Geophysical Research*, *107*(D3), AAC1-1–AAC1-6. https://doi.org/10.1029/2001JD000483

Albrecht, B. A. (1989). Aerosols, cloud microphysics, and fractional cloudiness. *Science*, *245*(4923), 1227–1230. https://doi.org/10.1126/science.245.4923.1227

Alexander, B., Park, R. J., Jacob, D. J., & Gong, S. (2009). Transition metal-catalyzed oxidation of atmospheric sulfur: Global implications for the sulfur budget. *Journal of Geophysical Research*, *114*(D2). https://doi.org/10.1029/2008JD010486

Allen, R. J., & Landuyt, W. (2014). The vertical distribution of black carbon in CMIP5 models: Comparison to observations and the importance of convective transport. *Journal of Geophysical Research: Atmospheres*, *119*(8), 4808–4835. https://doi.org/10.1002/2014JD021595

Archer-Nicholls, S., Lowe, D., Utembe, S., Allan, J., Zaveri, R. A., Fast, J. D., et al. (2014). Gaseous chemistry and aerosol mechanism developments for version 3.5.1 of the online regional model, WRF-CHEM. *Geoscientific Model Development*, *7*(6), 2557–2579. https://doi.org/10.5194/gmd-7-2557-2014

Bellouin, N., Quaas, J., Gryspeerdt, E., Kinne, S., Stier, P., Watson-Parris, D., et al. (2020). Bounding global aerosol radiative forcing of climate change. *Reviews of Geophysics*, *58*(1), e2019RG000660. https://doi.org/10.1029/2019RG000660

Bian, H., Chin, M., Colarco, P. R., Apel, E. C., Blake, D. R., Froyd, K., et al. (2024). Observationally constrained analysis of sulfur cycle in the marine atmosphere with NASA atom measurements and aerocom model simulations. *Atmospheric Chemistry and Physics*, *24*(3), 1717–1741. https://doi.org/10.5194/acp-24-1717-2024

Boucher, O., & Lohmann, U. (1995). The sulfate-CCN-cloud albedo effect: A sensitivity study with two general circulation models. *Tellus B: Chemical and Physical Meteorology*, *47*(3), 281. https://doi.org/10.3402/tellusb.v47i3.16048

Buchholz, R. R., Emmons, L. K., Tilmes, S., & Team, T. C. D. (2019). CESM2.1/CAM-chem instantaneous output for boundary conditions [Dataset]. *UCAR/NCAR - Atmospheric Chemistry Observations and Modeling Laboratory*. https://doi.org/10.24381/cds.143582cf

Carslaw, K. S., Lee, L. A., Reddington, C. L., Pringle, K. J., Rap, A., Forster, P. M., et al. (2013). Large contribution of natural aerosols to uncertainty in indirect forcing. *Nature*, *503*(7474), 67–71. https://doi.org/10.1038/nature12674

Chen, Y., Haywood, J., Wang, Y., Malavelle, F., Jordan, G., Partridge, D., et al. (2022). Machine learning reveals climate forcing from aerosols is dominated by increased cloud cover. *Nature Geoscience*, *15*(8), 609–614. https://doi.org/10.1038/s41561-022-00991-6

Chin, M., Ginoux, P., Kinne, S., Torres, O., Holben, B. N., Duncan, B. N., et al. (2002). Tropospheric aerosol optical thickness from the gocart model and comparisons with satellite and sun photometer measurements. *Journal of the Atmospheric Sciences*, *59*(3), 461–483. https://doi.org/10.1175/1520-0469(2002)059<0461:TAOTFT>2.0.CO;2

Christensen, M. W., Gettelman, A., Cermak, J., Dagan, G., Diamond, M., Douglas, A., et al. (2022). Opportunistic experiments to constrain aerosol effective radiative forcing. *Atmospheric Chemistry and Physics*, *22*(1), 641–674. https://doi.org/10.5194/acp-22-641-2022

Copernicus Climate Change Service. (2017). ERA5: Fifth generation of ECMWF atmospheric reanalyses of the global climate [Dataset]. *Copernicus Climate Change Service Climate Data Store (CDS)*. https://doi.org/10.24381/cds.adbb2d47

Denier van der Gon, H., Hendriks, C., Kuenen, J., Segers, A. A., & Visschedijk, A. (2011). *Description of current temporal emission patterns and sensitivity of predicted AQ for temporal emission patterns* TNO Report, EU FP7 MACC deliverable report D_DEMIS_1.3 (Tech. Rep.). Princetonlaan 6, 3584 CB. TNO.

Dusek, U., Frank, G. P., Hildebrandt, L., Curtius, J., Schneider, J., Walter, S., et al. (2006). Size matters more than chemistry for cloud-nucleating ability of aerosol particles. *Science*, *312*(5778), 1375–1378. https://doi.org/10.1126/science.1125261

EEA. (2014). Emission trends of sulphur oxides [Data Visualization]. Retrieved from https://www.eea.europa.eu/data-and-maps/daviz/emission-trends-of-sulphur-oxides#tab-chart_1

Ekman, A. M. L. (2014). Do sophisticated parameterizations of aerosol-cloud interactions in CMIP5 models improve the representation of recent observed temperature trends? *Journal of Geophysical Research: Atmospheres*, *119*(2), 817–832. https://doi.org/10.1002/2013JD020511

Emmons, L. K., Walters, S., Hess, P. G., Lamarque, J.-F., Pfister, G. G., Fillmore, D., et al. (2010). Description and evaluation of the model for ozone and related chemical tracers, version 4 (MOZART-4). *Geoscientific Model Development*, *3*(1), 43–67. https://doi.org/10.5194/gmd-3-43-2010

Fiedler, S., van Noije, T., Smith, C. J., Boucher, O., Dufresne, J.-L., Kirkevåg, A., et al. (2023). Historical changes and reasons for model differences in anthropogenic aerosol forcing in CMIP6. *Geophysical Research Letters*, *50*(15), e2023GL104848. https://doi.org/10.1029/2023GL104848

Ghan, S. J., Leung, L. R., Easter, R. C., & Abdul-Razzak, H. (1997). Prediction of cloud droplet number in a general circulation model. *Journal of Geophysical Research*, *102*(D18), 21777–21794. https://doi.org/10.1029/97JD01810

Grell, G. A., & Dévényi, D. (2002). A generalized approach to parameterizing convection combining ensemble and data assimilation techniques. *Geophysical Research Letters*, *29*(14), 38-1–38-4. https://doi.org/10.1029/2002GL015311

Grell, G. A., Peckham, S. E., Schmitz, R., McKeen, S. A., Frost, G., Skamarock, W. C., & Eder, B. (2005). Fully coupled "online" chemistry within the WRF model. *Atmospheric Environment*, *39*(37), 6957–6975. https://doi.org/10.1016/j.atmosenv.2005.04.027

Grosvenor, D. P., & Wood, R. (2014). The effect of solar zenith angle on MODIS cloud optical and microphysical retrievals within marine liquid water clouds. *Atmospheric Chemistry and Physics*, *14*(14), 7291–7321. https://doi.org/10.5194/acp-14-7291-2014

Gryspeerdt, E., Goren, T., Sourdeval, O., Quaas, J., Mülmenstädt, J., Dipu, S., et al. (2019). Constraining the aerosol influence on cloud liquid water path. *Atmospheric Chemistry and Physics*, *19*(8), 5331–5347. https://doi.org/10.5194/acp-19-5331-2019

Gryspeerdt, E., Povey, A. C., Grainger, R. G., Hasekamp, O., Hsu, N. C., Mulcahy, J. P., et al. (2023). Uncertainty in aerosol–cloud radiative forcing is driven by clean conditions. *Atmospheric Chemistry and Physics*, *23*(7), 4115–4122. https://doi.org/10.5194/acp-23-4115-2023

Guenther, A. B., Jiang, X., Heald, C. L., Sakulyanontvittaya, T., Duhl, T., Emmons, L. K., & Wang, X. (2012). The model of emissions of gases and aerosols from nature version 2.1 (MEGAN2.1): An extended and updated framework for modeling biogenic emissions. *Geoscientific Model Development*, *5*(6), 1471–1492. https://doi.org/10.5194/gmd-5-1471-2012

Hodnebrog, O., Myhre, G., Jouan, C., Andrews, T., Forster, P. M., Jia, H., et al. (2024). Recent reductions in aerosol emissions have increased Earth's energy imbalance. *Communications Earth & Environment*, *5*(1), 1–9. https://doi.org/10.1038/s43247-024-01324-8

Hubanks, P., Platnick, S., King, M., & Ridgway, B. (2016). *MODIS atmosphere L3 gridded product algorithm theoretical basis document (ATBD) & users guide* (Tech. Rep.). NASA EOS.

Ilyinskaya, E., Schmidt, A., Mather, T. A., Pope, F. D., Witham, C., Baxter, P., et al. (2017). Understanding the environmental impacts of large fissure eruptions: Aerosol and gas emissions from the 2014–2015 holuhraun eruption (Iceland). *Earth and Planetary Science Letters*, *472*, 309–322. https://doi.org/10.1016/j.epsl.2017.05.025

Ioannidis, E., Law, K. S., Raut, J.-C., Marelle, L., Onishi, T., Kirpes, R. M., et al. (2023). Modelling wintertime sea-spray aerosols under arctic haze conditions. *Atmospheric Chemistry and Physics*, *23*(10), 5641–5678. https://doi.org/10.5194/acp-23-5641-2023

IPCC. (2023). The Earth's energy budget, climate feedbacks and climate sensitivity. In *Climate Change 2021—The Physical Science Basis: Working Group I Contribution to the Sixth Assessment Report of the Intergovernmental Panel on Climate Change* (pp. 923–1054). Cambridge University Press.

Lana, A., Bell, T. G., Simó, R., Vallina, S. M., Ballabrera-Poy, J., Kettle, A. J., et al. (2011). An updated climatology of surface dimethlysulfide concentrations and emission fluxes in the global ocean. *Global Biogeochemical Cycles*, *25*(1). https://doi.org/10.1029/2010GB003850

Lapere, R., Thomas, J. L., Marelle, L., Ekman, A. M. L., Frey, M. M., Lund, M. T., et al. (2023). The representation of sea salt aerosols and their role in polar climate within CMIP6. *Journal of Geophysical Research: Atmospheres*, *128*(6), e2022JD038235. https://doi.org/10.1029/2022JD038235

Li, G., Wieder, J., Pasquier, J. T., Henneberger, J., & Kanji, Z. A. (2022). Predicting atmospheric background number concentration of ice-nucleating particles in the Arctic. *Atmospheric Chemistry and Physics*, *22*(21), 14441–14454. https://doi.org/10.5194/acp-22-14441-2022

Lohmann, U., & Feichter, J. (2005). Global indirect aerosol effects: A review. *Atmospheric Chemistry and Physics*, *5*(3), 715–737. https://doi.org/10.5194/acp-5-715-2005

Lohmann, U., Feichter, J., Penner, J., & Leaitch, R. (2000). Indirect effect of sulfate and carbonaceous aerosols: A mechanistic treatment. *Journal of Geophysical Research*, *105*(D10), 12193–12206. https://doi.org/10.1029/1999JD901199

Lohmann, U., Lüönd, F., & Mahrt, F. (2016). *An introduction to clouds: From the microscale to climate*. Cambridge University Press. https://doi.org/10.1017/CBO9781139087513

Madeleine, J.-B., Hourdin, F., Grandpeix, J.-Y., Rio, C., Dufresne, J.-L., Vignon, E., et al. (2020). Improved representation of clouds in the atmospheric component LMDZ6A of the IPSL-CM6A Earth system model. *Journal of Advances in Modeling Earth Systems*, *12*(10), e2020MS002046. https://doi.org/10.1029/2020MS002046

Mahfouz, N., Mülmenstädt, J., & Burrows, S. (2024). Present-day correlations are insufficient to predict cloud albedo change by anthropogenic aerosols in E3SM v2. *Atmospheric Chemistry and Physics*, *24*(12), 7253–7260. https://doi.org/10.5194/acp-24-7253-2024

Malavelle, F. F., Haywood, J. M., Jones, A., Gettelman, A., Clarisse, L., Bauduin, S., et al. (2017). Strong constraints on aerosol–cloud interactions from volcanic eruptions. *Nature*, *546*(7659), 485–491. https://doi.org/10.1038/nature22974

Marelle, L. (2024a). WRF 4.3.3 model version with additional developments for aerosol-cloud interactions [Software]. *Zenodo*. https://doi.org/10.5281/zenodo.12544534

Marelle, L. (2024b). WRF-Chem run scripts and postprocessing scripts for the aerosol-cloud study of the Holuhraun eruption [Software]. *Zenodo*. https://doi.org/10.5281/zenodo.12544354

Marelle, L., Raut, J.-C., Law, K. S., Berg, L. K., Fast, J. D., Easter, R. C., et al. (2017). Improvements to the WRF-CHEM 3.5.1 model for quasi-hemispheric simulations of aerosols and ozone in the Arctic. *Geoscientific Model Development*, *10*(10), 3661–3677. https://doi.org/10.5194/gmd-10-3661-2017

McCoy, D. T., Field, P., Gordon, H., Elsaesser, G. S., & Grosvenor, D. P. (2020). Untangling causality in midlatitude aerosol–cloud adjustments. *Atmospheric Chemistry and Physics*, *20*(7), 4085–4103. https://doi.org/10.5194/acp-20-4085-2020

McCoy, D. T., Field, P. R., Schmidt, A., Grosvenor, D. P., Bender, F. A.-M., Shipway, B. J., et al. (2018). Aerosol midlatitude cyclone indirect effects in observations and high-resolution simulations. *Atmospheric Chemistry and Physics*, *18*(8), 5821–5846. https://doi.org/10.5194/acp-18-5821-2018

McCoy, D. T., & Hartmann, D. L. (2015). Observations of a substantial cloud-aerosol indirect effect during the 2014–2015 Bárðarbunga-Veiðivötn fissure eruption in Iceland. *Geophysical Research Letters*, *42*(23), 10409–10414. https://doi.org/10.1002/2015GL067070

McCoy, I. L., McCoy, D. T., Wood, R., Regayre, L., Watson-Parris, D., Grosvenor, D. P., et al. (2020). The hemispheric contrast in cloud microphysical properties constrains aerosol forcing. *Proceedings of the National Academy of Sciences of the United States of America*, *117*(32), 18998–19006. https://doi.org/10.1073/pnas.1922502117

Mülmenstädt, J., & Feingold, G. (2018). The radiative forcing of aerosol–cloud interactions in liquid clouds: Wrestling and embracing uncertainty. *Current Climate Change Reports*, *4*(1), 23–40. https://doi.org/10.1007/s40641-018-0089-y

Mülmenstädt, J., Gryspeerdt, E., Dipu, S., Quaas, J., Ackerman, A. S., Fridlind, A. M., et al. (2024). General circulation models simulate negative liquid water path–droplet number correlations, but anthropogenic aerosols still increase simulated liquid water path. *EGUsphere*, *2024*(12), 1–29. https://doi.org/10.5194/egusphere-2024-4

Nightingale, P. D., Malin, G., Law, C. S., Watson, A. J., Liss, P. S., Liddicoat, M. I., et al. (2000). In situ evaluation of air-sea gas exchange parameterizations using novel conservative and volatile tracers. *Global Biogeochemical Cycles*, *14*(1), 373–387. https://doi.org/10.1029/1999GB900091

Pfeffer, M. A., Bergsson, B., Barsotti, S., Stefánsdóttir, G., Galle, B., Arellano, S., et al. (2018). Ground-based measurements of the 2014–2015 holuhraun volcanic cloud (Iceland). *Geosciences*, *8*(1), 29. https://doi.org/10.3390/geosciences8010029

Platnick, S., et al. (2015a). MODIS atmosphere L3 monthly product [Dataset]. *NASA MODIS Adaptive Processing System, Goddard Space Flight Center, USA*. https://doi.org/10.5067/MODIS/MYD08_M3.061

Platnick, S., et al. (2015b). MODIS atmosphere L3 monthly product [Dataset]. *NASA MODIS Adaptive Processing System, Goddard Space Flight Center, USA*. https://doi.org/10.5067/MODIS/MOD08_M3.061

Quaas, J., Arola, A., Cairns, B., Christensen, M., Deneke, H., Ekman, A. M. L., et al. (2020). Constraining the twomey effect from satellite observations: Issues and perspectives. *Atmospheric Chemistry and Physics*, *20*(23), 15079–15099. https://doi.org/10.5194/acp-20-15079-2020

Quaas, J., Jia, H., Smith, C., Albright, A. L., Aas, W., Bellouin, N., et al. (2022). Robust evidence for reversal of the trend in aerosol effective climate forcing. *Atmospheric Chemistry and Physics*, *22*(18), 12221–12239. https://doi.org/10.5194/acp-22-12221-2022

Schmidt, A., Leadbetter, S., Theys, N., Carboni, E., Witham, C. S., Stevenson, J. A., et al. (2015). Satellite detection, long-range transport, and air quality impacts of volcanic sulfur dioxide from the 2014–2015 flood lava eruption at Bárðarbunga (Iceland). *Journal of Geophysical Research: Atmospheres*, *120*(18), 9739–9757. https://doi.org/10.1002/2015JD023638

Seinfeld, J. H., Bretherton, C., Carslaw, K. S., Coe, H., DeMott, P. J., Dunlea, E. J., et al. (2016). Improving our fundamental understanding of the role of aerosol-cloud interactions in the climate system. *Proceedings of the National Academy of Sciences of the United States of America*, *113*(21), 5781–5790. https://doi.org/10.1073/pnas.1514043113

Tegen, I., Hollrig, P., Chin, M., Fung, I., Jacob, D., & Penner, J. (1997). Contribution of different aerosol species to the global aerosol extinction optical thickness: Estimates from model results. *Journal of Geophysical Research*, *102*(D20), 23895–23915. https://doi.org/10.1029/97JD01864

Thompson, G., & Eidhammer, T. (2014). A study of aerosol impacts on clouds and precipitation development in a large winter cyclone. *Journal of the Atmospheric Sciences*, *71*(10), 3636–3658. https://doi.org/10.1175/JAS-D-13-0305.1

Twomey, S. (1974). Pollution and the planetary albedo. *Atmospheric Environment*, *8*(12), 1251–1256. https://doi.org/10.1016/0004-6981(74)90004-3

van der Gon, H. D., Gauss, M., Granier, C., Arellano, S., Benedictow, A., Darras, S., et al. (2023). Copernicus atmosphere monitoring Service regional emissions version 4.2 (CAMS-REG-v4.2) [Dataset]. *Copernicus Atmosphere Monitoring Service*. https://doi.org/10.24380/q2si-ti6i

von Glasow, R., & Crutzen, P. J. (2004). Model study of multiphase dms oxidation with a focus on halogens. *Atmospheric Chemistry and Physics*, *4*(3), 589–608. https://doi.org/10.5194/acp-4-589-2004

von Salzen, K., Whaley, C. H., Anenberg, S. C., Van Dingenen, R., Klimont, Z., Flanner, M. G., et al. (2022). Clean air policies are key for successfully mitigating Arctic warming. *Communications Earth & Environment*, *3*(1), 1–11. https://doi.org/10.1038/s43247-022-00555-x

Wiedinmyer, C., Yokelson, R. J., & Gullett, B. K. (2014). Global emissions of trace gases, particulate matter, and hazardous air pollutants from open burning of domestic waste. *Environmental Science and Technology*, *48*(16), 9523–9530. https://doi.org/10.1021/es502250z

Xu, K.-M., & Randall, D. A. (1996). A semiempirical cloudiness parameterization for use in climate models. *Journal of the Atmospheric Sciences*, *53*(21), 3084–3102. https://doi.org/10.1175/1520-0469(1996)053<3084:ASCPFU>2.0.CO;2

Zaveri, R. A., Easter, R. C., Fast, J. D., & Peters, L. K. (2008). Model for simulating aerosol interactions and chemistry (MOSAIC). *Journal of Geophysical Research*, *113*(D13). https://doi.org/10.1029/2007JD008782

Zelinka, M. D., Smith, C. J., Qin, Y., & Taylor, K. E. (2023). Comparison of methods to estimate aerosol effective radiative forcings in climate models. *Atmospheric Chemistry and Physics*, *23*(15), 8879–8898. https://doi.org/10.5194/acp-23-8879-2023

References From the Supporting Information

Iacono, M. J., Delamere, J. S., Mlawer, E. J., Shephard, M. W., Clough, S. A., & Collins, W. D. (2008). Radiative forcing by long-lived greenhouse gases: Calculations with the aer radiative transfer models. *Journal of Geophysical Research*, *113*(D13). https://doi.org/10.1029/2008JD009944

Nakanishi, M., & Niino, H. (2009). Development of an improved turbulence closure model for the atmospheric boundary layer. *Journal of the Meteorological Society of Japan Series II*, *87*(5), 895–912. https://doi.org/10.2151/jmsj.87.895

Tewari, M., Chen, F., Wang, W., Dudhia, J., LeMone, M. A., Gayno, G., et al. (2004). Implementation and verification of the unified Noah land surface model in the WRF model. In *20th Conference on Weather Analysis and Forecasting/16th Conference on Numerical Weather Prediction* (pp. 11–15).